

# Higher-order ferromagnetic resonances in periodic arrays of synthetic-antiferromagnet nanodiscs

V. Yu. Borynskyi,<sup>1</sup> D. M. Polishchuk,<sup>1,2</sup> A. K. Melnyk,<sup>3</sup> A. F. Kravets,<sup>1,2</sup> A. I. Tovstolytkin,<sup>1</sup> and V. Korenivski<sup>2</sup>

<sup>1</sup>*Institute of Magnetism of NAS of Ukraine and MES of Ukraine, 36-b Akad. Vernadskyi blvd., Kyiv 03142, Ukraine*

<sup>2</sup>*Nanostructure Physics, Royal Institute of Technology, Stockholm 10691, Sweden*

<sup>3</sup>*Institute for Sorption and Problems of Endoecology of NAS of Ukraine, 13 Naumov str., Kyiv 03164, Ukraine*

We investigate spin dynamics in nanodisc arrays of synthetic-antiferromagnets (SAF) made of Py/NiCu/Py trilayers, where the NiCu spacer undergoes a Curie transition at about 200 K. The observed ferromagnetic resonance spectra have three distinct resonance modes at room temperature, which are fully recreated in our micromagnetic simulations showing also how the intra-SAF asymmetry can be used to create and control the higher-order resonances in the structure. Below the Curie temperature of the spacer, the system effectively transitions into a single-layer nanodisc array with only two resonance modes. Our results show how multi-layering of nano-arrays can add tunable GHz functionality relevant for such rapidly developing fields as magnetic metamaterials, magnonic crystals, arrays of spin-torque oscillators and neuromorphic junctions.

The last decade has seen large research efforts focused on collective spin dynamics of magnonic crystals and logic circuits aimed for various high-speed applications [1–4]. Controllable size of the individual elements used in such metamaterials, down to the 10 nm range, enables rich higher-order FMR dynamics such as standing spin waves and edge-mode resonances. The typical geometry of a periodic array offers high flexibility in engineering novel properties. At the same time, the increased complexity requires systematic investigations of various effects and parameters involved [5–8].

Relatively simple periodic arrays of single-layer ferromagnetic nanodiscs exhibit anisotropic spin wave modes (commonly, with four-fold in-plane anisotropy) affected by the inter-element dipolar interactions [9–11]. The properties become more intriguing for arrays of multilayered elements such as SAF's, which are of interest in antiferromagnetic spintronics [12] as well as magnonics [13]. Their collective spin dynamics is dictated by the inter-element interactions, the intra-particle dipolar coupling, and the interplay of the two [14–16].

Arrays of multilayered nanomagnets can exhibit distinct spin dynamic modes not found in single-layer systems. The intra-particle dipolar interactions lead to complex demagnetizing field distributions, altering the collective spin dynamics in such systems, resulting in mode-frequency shifts [17] or even splitting of the resonant modes [18]. For example, a systematic micromagnetic study performed by Pauselli *et al.* [14] for a sub-40-nm magnetic tunnel junction read head explained additional higher-order modes as originating from a strong localization of spin excitations to the junction's edges, where an excitation in one of the junction's magnetic layers drives a localized resonance in the neighboring, dipole-coupled magnetic layer. Multi-layering is thus a capable tool for varying spin wave modes and therefore spectral modification [19, 20], additional to element grouping or sequencing in arrays of single-layer nanoparticles [18, 21]. Furthermore, particle shape imperfections unavoidable on the experiment, such as edge deviations [22] or a sidewall angle [23], can have a significant effect on the spin dynamics of the system. Strongly localized edge-mode excitations are highly sensitive to this kind of distortions, which can lead to lifting of their degeneracy for both single-layer [24] and multilayered [25] systems. While arrays of single-layer nanoparticles are well

studied [26–28], a systematic investigation of arrays of multilayered nano-elements is still pending.

In this work, we investigate higher-order FMR excitations in periodic arrays of multilayered SAF nanodiscs, designed with an in-situ thermal control of the interlayer coupling capable of making the nanodiscs effectively single-layered. This in-situ control of the SAF versus single-layer character of the array elements allows us to identify the SAF-unique properties from a direct comparison of the FMR spectra measured above and below the Curie point of the spacer. Using detailed micromagnetic simulations, we explain the occurrence, positions, and anisotropy of the measured resonances and how they are affected by strong localizations of the spin excitations and a complex interplay between the inter- and intra-particle interactions, pronounced in SAF-based nanostructures.

We focus our investigation on arrays of SAF nanodiscs Py(7 nm)/NiCu(10 nm)/Py(7 nm) with periodicity 250 nm and nominal diameter  $d = 150$  nm. Here, Py and NiCu stand for Ni<sub>80</sub>Fe<sub>20</sub> (Permalloy) and Ni<sub>60</sub>Cu<sub>40</sub>, respectively. The spacer is paramagnetic at room temperature (RT) and mediates no direct exchange between the outer Py layers, which interact through magnetostatic coupling only, thereby forming a SAF element. At low temperature, the spacer is ferromagnetic, which allows in-situ switching between the SAF and the single-layer states in the system [29, 30]. Multilayers Py/NiCu/Py were grown by magnetron sputtering (Orion, AJA Int.) onto thermally oxidized Si (001) wafers at room temperature. The multilayers were then used to fabricate arrays of SAF nanodiscs using electron-beam lithography (Voyager, Raith Inc.). The arrays were etched using Ar-plasma via a double-layer hard mask, TaN(60 nm)/Al(20 nm). Here, thin Al was used as a lift-off layer to form a mask (with the nominal diameter  $d_0 = 150$  nm) for selective reactive plasma etching with SF<sub>6</sub> of the thick TaN layer underneath. Additional array geometries were fabricated and tested for calibration and verification purposes, in the process of optimizing the SAF arrays, with most interesting properties presented herein.

SEM images of the fabricated arrays in Fig. 1(a–b) show good uniformity in the element size (the spread is less than 5 %) and good edge morphology. Angled SEM in Fig. 1(b) shows a side-wall angle of 20–30°, formed in the process of plasma etching, making the effective diameter of the top Py

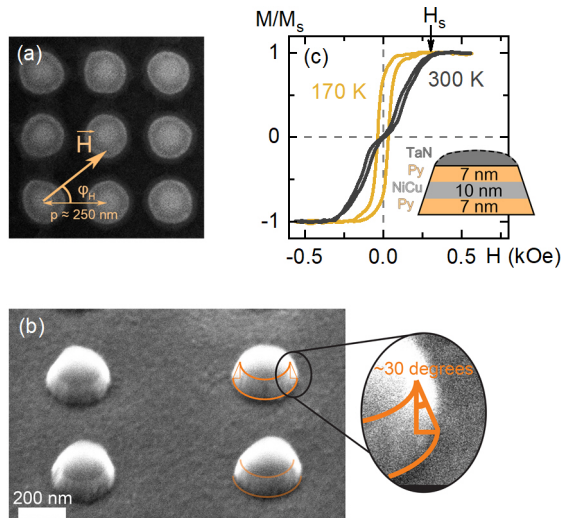


FIG. 1. (a) Top-view SEM image of select region in planar array of 150-nm SAF nanodiscs (Py/NiCu/Py). Inset indicates particle periodicity and in-plane orientation of external magnetic field. (b) 45° SEM view of same sample. (c) Typical M-H loops, measured using MOKE at 300 and 170 K; inset illustrates vertical cross-section of single SAF nanodisc. TaN is used as etching mask and for capping.

disc about 15 % smaller than that of the bottom disc. The top dome-like cap, visible as the central concentric circles in the top-view and contrasted-top in the side-view SEM images, Fig. 1(a–b), is the remaining TaN mask that protects the fabricated particles from oxidation.

Cavity-FMR measurements were carried out using an X-band ELEXSYS E500 spectrometer (Bruker Inc.) equipped with an automatic goniometer for precise angle control. The measurements were performed at a constant operating frequency of 9.36 GHz. The magnetic volume of the arrays of area  $1.4 \times 1.4$  mm<sup>2</sup> was large enough for a high signal-to-noise ratio. Additionally, magnetostatic properties of the arrays were measured using a custom-made variable-temperature magneto-optical Kerr-effect (MOKE) setup.

Figure 1(c) shows two characteristic MOKE loops measured in-plane ( $\phi_H = 0^\circ$ ). Zero remnant magnetization at  $H = 0$  and relatively high saturation field  $H_s \approx 300$  Oe for RT loop indicate a pronounced antiferromagnetic-type interlayer coupling of the top and bottom magnetic moments of the individual SAF nanodiscs. The double-step shape and small hysteresis can arise from the presence of magnetic anisotropy [31] as well as a non-ideal circular shape of the nanodiscs [32, 33].

Figure 2(a) shows the FMR spectra measured at RT for the array of 150-nm SAF nanodiscs with different in-plane orientations of the external magnetic field,  $\phi_H = 0, 45,$  and  $90^\circ$ . Each curve shows three well-defined resonance lines marked as  $L_m$ ,  $L_{e1}$ , and  $L_{e2}$ . We associate the  $L_m$  line with the quasi-uniform (hereafter *main*) FMR mode since its position coincides with that of the resonance line for a continuous Py film. With respect to the position of  $L_m$ , lines  $L_{e1}$  and  $L_{e2}$  are observed at higher resonance fields. A similar

higher-field mode, along with the main mode, was reported previously [11] for arrays of single-layer nanodiscs and was attributed to the edge-mode resonance. For our arrays of SAF nanodiscs, we observe two higher-field modes, both of which we associate with higher-order edge-mode resonances in the SAF nanostructure – the interpretation supported by our micromagnetic simulations, detailed below. We note that any FMR modes related to potential domains or vortices forming in the SAF particles are excluded from consideration since the resonance fields of  $L_m$ ,  $L_{e1}$ , and  $L_{e2}$  ( $H_r > 1$  kOe) are much higher than the SAF saturation field [ $H_s \approx 300$  Oe; Fig. 1(c)].

The resonance field,  $H_r$ , of each resonance line show a pronounced angular dependence, as seen in Fig. 2(b). All lines show bi-axial anisotropy with, however, opposite hard and easy axes for  $L_m$  and  $L_{e1,e2}$ . While  $L_m$  exhibits easy axes (minimum  $H_r$ ) at  $45^\circ$  with respect to the main  $x$  and  $y$  axes of the array [Fig. 1(a)], the edge-modes,  $L_{e1}$  and  $L_{e2}$ , have easy axes along  $x$  and  $y$ . Such anisotropic behavior was explained in Refs. 9 and 34 by the inter-element dipole coupling leading to a non-uniform effective field distribution within the individual discs, even at rather high external fields.

In order to explain the origin and behavior of the three FMR modes observed, we performed detailed micromagnetic simulations [35], using MuMax3 [36, 37]. The layout of each element as well as the base diameter ( $d_0$ ) used were those observed experimentally [Fig. 1(c)]. Figure 2(c) displays the calculated spectra for two isolated single-layer Py discs (7 nm thick) with diameters  $d_0 = 150$  nm (blue line) and  $d = 0.85d_0$  (red dashed line). This difference in size corresponds to the SEM-measured difference in the diameters of the bottom and top layers of our SAF nanodiscs; cf. Fig. 1(b). Both simulated spectra show two resonance lines corresponding to the main and edge-resonance modes, illustrated by the insets to Fig. 2(c). Of note is that despite line  $L_m$  is associated with the uniform mode of a continuous Py film, the related excitation within a nanodisc is not fully spatially uniform, which is why we call it *main* rather than *uniform* FMR mode. Importantly, neither spectrum shows any trace of a third line observed on the experiment, nor a related additional line can be obtained when the two spectra are superposed.

The simulated spectra are substantially different when the two discs of  $d_0 = 150$  nm and  $d = 0.85d_0$  form a SAF element, as shown in Fig. 2(d). Three resonance lines are visible, with the positions and intensities resembling the experimental data. The insets to Fig. 2(d) clarify why we associate the high-field lines with edge-mode resonances. Whereas the  $L_{e1}$  mode is excited mostly in the bottom layer, the  $L_{e2}$  mode is more intensive in the top layer. Importantly, when the top and bottom layers are of equal diameter, only two modes,  $L_m$  and  $L_{e1}$ , are excited; the third mode appears only when the top and bottom diameters become noticeably different (by 5–10 %).

Figure 2(e) shows the simulated angle-dependence of the resonance fields of the  $L_m$ ,  $L_{e1}$ , and  $L_{e2}$  modes obtained for an array of SAF nanodiscs. The simulations are in excellent agreement with the experimental resonance-field versus angle data of Fig. 2(b), which further validates our interpretation of the observed modes and their properties.

Figure 3(a) compares the SAF FMR spectra measured as

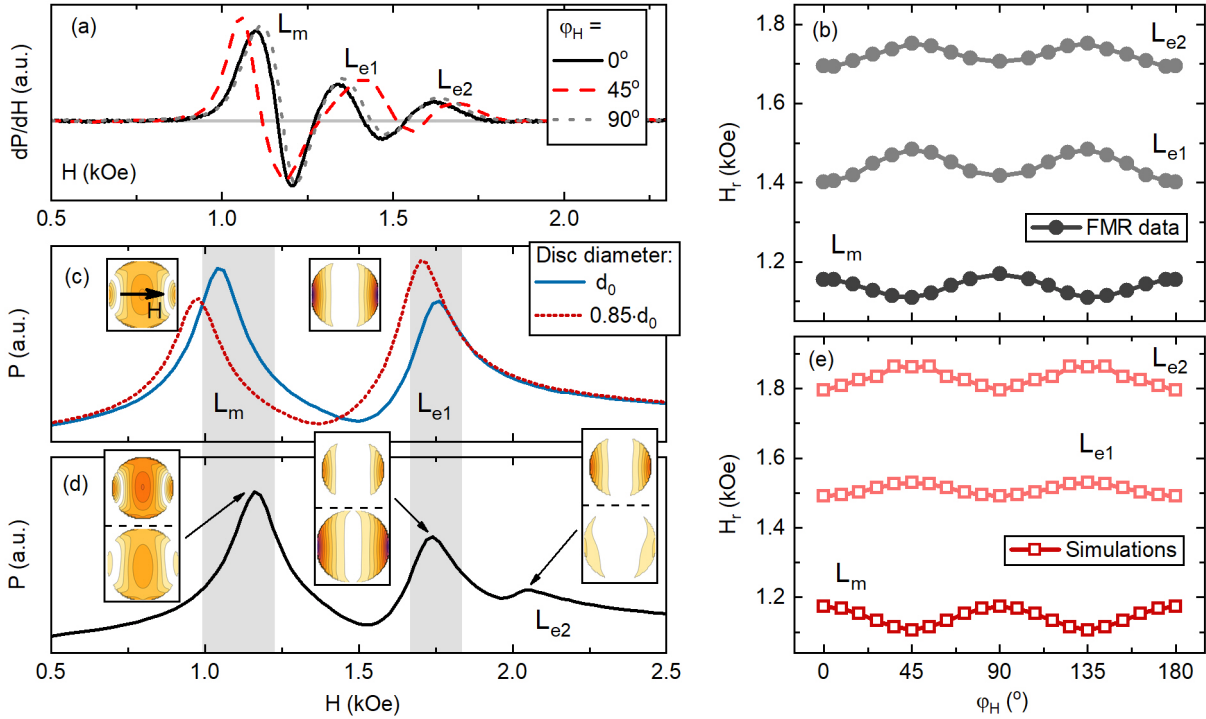


FIG. 2. (a) FMR spectra measured at RT for 150-nm SAF array at 0, 45, and  $90^\circ$ -oriented external field.  $L_m$ ,  $L_{e1}$  and  $L_{e2}$  mark resonance lines attributed to main and two edge-modes, respectively. (b) Resonance fields of individual modes versus in-plane angle. (c) FMR spectra calculated for individual single-layer discs with  $d_0 = 150$  nm and  $d \approx 0.85d_0$ , corresponding to bottom and top layers of SAF nanodiscs. Insets show excitation regions for two eigen-modes. (d) Calculated FMR spectrum for individual SAF particle with  $d_0$  and  $d \approx 0.85d_0$ . Insets display excitation regions in both layers of SAF nanodisc. All spectra were calculated with in-plane field at  $\phi_H = 0^\circ$  (black arrow in left inset to c). (e) In-plane angular dependence of resonance fields simulated for SAF disc array with  $d_0 = 150$  nm,  $d \approx 0.85d_0$ , and array periodicity 200 nm.

the temperature is lowered from room to below the Curie point of the NiCu spacer. Our SAF design is rather unique as it effectively transforms the nano-elements from trilayers to single-layers when the spacer transitions from para- to ferromagnetic state at about 220 K [29, 30, 38, 39]. The associated transition in the FMR spectrum is very illuminating – the three-mode resonance is reduced to effectively two modes, which is a known characteristic of single-layer nano-arrays. Figure 3(b) shows the fits to the extracted high-order resonances (after subtracting the main peak): the pronounced double-resonance at room temperature with dominating  $L_{e1}$  (red) and essentially a single broad peak at 170 K where the  $L_{e1}$  peak is  $<1\%$  of its RT value. The transition from two high-order peaks to one takes place precisely at the Curie temperature of the spacer, deduced independently from our MOKE magnetization data shown in Fig. 3(c). We thus confirm, in a direct experiment, that the origin of the double spin-wave resonance is unique to SAF nano-arrays. Specifically, the high-order (non-uniform) double resonance is a result of hybridization of predominantly acoustic and optical (in-phase and out-phase) oscillations in the two ferromagnetic layers comprising the SAF. These modes collapse into one on direct exchange coupling the outer layers below the  $T_C$  of the spacer and, generally, can be tuned by changing the SAF geometry and the spacer properties (via magnetic dilution and/or temperature).

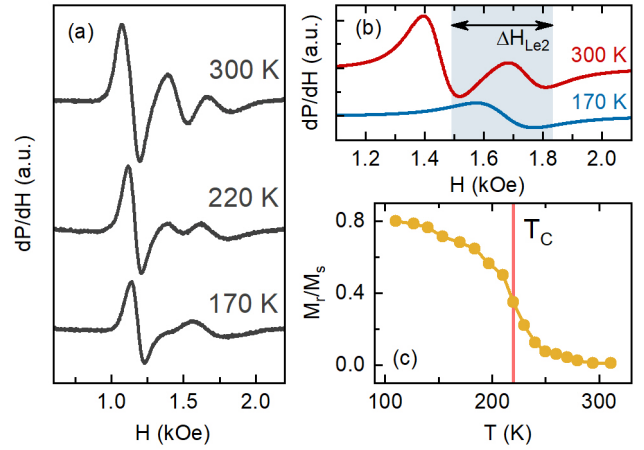


FIG. 3. (a) FMR spectra of SAF arrays measured at select temperatures. (b) Fits of high-order resonances ( $L_{e1}, L_{e2}$ ) at above and below spacer's Curie point. (c) Normalized remnant magnetization versus temperature obtained from MOKE loops.

The above results demonstrate that the magnetization dynamics of periodic arrays of SAF nanomagnets have key distinctions from the known behavior of single-layered nano-

arrays. Our variable field-angle and temperature FMR and MOKE studies, supported by morphological characterization and micromagnetic simulations, enable us to identify the origins of the distinct SAF properties observed. The three FMR modes and their pronounced in-plane anisotropy are two such distinct properties that, however, are governed by different factors. Our micromagnetic simulations indicate that the splitting of the higher-order edge mode into two is due to the dipolar coupling within the individual, asymmetric SAF particles. Here, the inter-particle interaction within the array is a secondary effect, which on the other hand dominates the anisotropic properties of the array. We find that the high-order spin excitations are hybridized acoustic (predominantly in-phase for  $L_{e1}$ ) and optical (predominantly out-of-phase for  $L_{e2}$ ) oscillations in the two layers comprising the SAF.

The occurrence of similar edge modes in single-layer nanodiscs is usually explained by a non-uniform internal field distribution, with its minima located at the edges orthogonal to the static magnetization of the discs [14]. Following similar logic for our asymmetric SAFs, we associate the two edge resonances with non-uniform field distributions that are different in each of the two nanodiscs owing to their different internal and external (inter-layer) demagnetization field profiles. The demagnetization is stronger in the smaller-diameter top layer, which results in a higher external field needed to excite the edge mode in this layer. In a symmetric SAF, with symmetric demagnetization fields, only one edge mode is excited.

The four-fold anisotropy of the three FMR modes is due to the bi-axial symmetry of our periodic arrays forming a square lattice. For our circular 150-nm SAF nanodisc arrays, this anisotropy is clearly caused by the inter-particle dipolar inter-

actions. The observed 45°-angle between the easy axes of the main mode and the edge modes can be explained by the difference in the spacing of the respective excitation nodes for single-layer nanodot arrays [34]. We are able to recreate this type of anisotropy in our micromagnetic simulations of SAF nano-arrays (to be discussed elsewhere).

In summary, we have investigated experimentally and micromagnetically the spin dynamics of arrays of three-layer SAF nanoparticles where the intra-SAF coupling can be in-situ controlled by varying temperature. The results show how the intra- and inter-particle dipolar interactions combine to produce rather unique GHz properties of the system, such as additional spin-wave modes that can be tuned by the SAF geometry and/or temperature, which are relevant for the emerging field of nanostructured magnetic metamaterials and magnonic devices.

## ACKNOWLEDGMENTS

We thank Dr. Roman Verba for fruitful discussions. Support from the Swedish Research Council (VR 2018-03526), the Olle Engkvist Foundation (2020-207-0460), the Volkswagen Foundation (90418), and the National Academy of Sciences of Ukraine (Projects 0119U100469, and 0120U100457) are gratefully acknowledged.

## DATA AVAILABILITY

The data supporting the findings of this study are available from the corresponding author upon request.

- 
- [1] A. V. Chumak, V. I. Vasyuchka, A. A. Serga, and B. Hillebrands, “Magnon spintronics,” *Nature Physics* **11**, 453–461 (2015).
- [2] X. M. Liu, J. Ding, G. N. Kakazei, and A. O. Adeyeye, “Magnonic crystals composed of Ni80Fe20 film on top of Ni80Fe20 two-dimensional dot array,” *Applied Physics Letters* **103**, 062401 (2013).
- [3] B. Lenk, H. Ulrichs, F. Garbs, and M. Münzenberg, “The building blocks of magnonics,” *Physics Reports* **507**, 107–136 (2011).
- [4] Arabinda Haldar and Adekunle Olusola Adeyeye, “Deterministic control of magnetization dynamics in reconfigurable nanomagnetic networks for logic applications,” *ACS Nano* **10**, 1690–1698 (2016).
- [5] Susmita Saha, Ruma Mandal, Saswati Barman, Dheeraj Kumar, Bivas Rana, Yasuhiro Fukuma, Satoshi Sugimoto, YoshiChika Otani, and Anjan Barman, “Tunable magnonic spectra in two-dimensional magnonic crystals with variable lattice symmetry,” *Advanced Functional Materials* **23**, 2378–2386 (2012).
- [6] Zhigang Liu, Richard D. Sydora, and Mark R. Freeman, “Shape effects on magnetization state transitions in individual 160-nm diameter Permalloy disks,” *Physical Review B* **77**, 174410 (2008).
- [7] M. L. Schneider, J. M. Shaw, A. B. Kos, Th. Gerrits, T. J. Silva, and R. D. McMichael, “Spin dynamics and damping in nanomagnets measured directly by frequency-resolved magneto-optic Kerr effect,” *Journal of Applied Physics* **102**, 103909 (2007).
- [8] R. V. Verba, E. G. Galkina, V. S. Tiberkevich, A. N. Slavin, and B. A. Ivanov, “Spin-wave modes localized on isolated defects in a two-dimensional array of dipolarly coupled magnetic nanodots,” *Physical Review B* **102**, 054421 (2020).
- [9] C. Mathieu, C. Hartmann, M. Bauer, O. Buettner, S. Riedling, B. Roos, S. O. Demokritov, B. Hillebrands, B. Bartenlian, C. Chappert, D. Decanini, F. Rousseaux, E. Cambri, A. Müller, B. Hoffmann, and U. Hartmann, “Anisotropic magnetic coupling of permalloy micron dots forming a square lattice,” *Applied Physics Letters* **70**, 2912–2914 (1997).
- [10] G. N. Kakazei, Yu. G. Pogorelov, M. D. Costa, T. Mewes, P. E. Wigen, P. C. Hammel, V. O. Golub, T. Okuno, and V. Novosad, “Origin of fourfold anisotropy in square lattices of circular ferromagnetic dots,” *Physical Review B* **74**, 060406 (2006).
- [11] Giovanni Carlotti, “Pushing down the lateral dimension of single and coupled magnetic dots to the nanometric scale: Characteristics and evolution of the spin-wave eigenmodes,” *Applied Physics Reviews* **6**, 031304 (2019).
- [12] R. A. Duine, Kyung-Jin Lee, Stuart S. P. Parkin, and M. D. Stiles, “Synthetic antiferromagnetic spintronics,” *Nature Physics* **14**, 217–219 (2018).
- [13] Arezoo Etesamirad, Rodolfo Rodriguez, Joshua Bocanegra, Roman Verba, Jordan Katine, Ilya N. Krivorotov, Vasyly Tyberkevych, Boris Ivanov, and Igor Barsukov, “Controlling

- magnon interaction by a nanoscale switch,” *ACS Applied Materials & Interfaces* **13**, 20288–20295 (2021).
- [14] Maurizio Pauselli, Andrzej A. Stankiewicz, and Giovanni Carlotti, “Linear and non-linear dynamics of the free and reference layers in a sub-40 nm magnetic tunnel junction: a micromagnetic study,” *Journal of Physics D: Applied Physics* **50**, 455007 (2017).
- [15] A. Kamimaki, S. Iihama, K. Z. Suzuki, N. Yoshinaga, and S. Mizukami, “Parametric amplification of magnons in synthetic antiferromagnets,” *Physical Review Applied* **13**, 044036 (2020).
- [16] Jyotirmoy Chatterjee, Stephane Auffret, Ricardo Sousa, Paulo Coelho, Ioan-Lucian Prejbeanu, and Bernard Dieny, “Novel multifunctional RKKY coupling layer for ultrathin perpendicular synthetic antiferromagnet,” *Scientific Reports* **8**, 1–9 (2018).
- [17] A. Talapatra and A. O. Adeyeye, “Coupled magnetic nanostructures: Engineering lattice configurations,” *Applied Physics Letters* **118**, 172404 (2021).
- [18] G. Carlotti, S. Tacchi, G. Gubbiotti, M. Madami, H. Dey, G. Csaba, and W. Porod, “Spin wave eigenmodes in single and coupled sub-150 nm rectangular permalloy dots,” *Journal of Applied Physics* **117**, 17A316 (2015).
- [19] Arabinda Haldar and Adekunle Olusola Adeyeye, “Reconfigurable and self-biased magnonic metamaterials,” *Journal of Applied Physics* **128**, 240902 (2020).
- [20] Krishna Begari and Arabinda Haldar, “Bias-free giant tunability of microwave properties in multilayer rhomboid nanomagnets,” *Journal of Physics D: Applied Physics* **51**, 275004 (2018).
- [21] Jack C. Gartside, Alex Vanstone, Troy Dion, Kilian D. Stenning, Daan M. Arroo, Hidekazu Kurebayashi, and Will R. Branford, “Reconfigurable magnonic mode-hybridisation and spectral control in a bicomponent artificial spin ice,” *Nature Communications* **12**, 1–9 (2021).
- [22] H. T. Nembach, R. D. McMichael, M. L. Schneider, J. M. Shaw, and T. J. Silva, “Comparison of measured and simulated spin-wave mode spectra of magnetic nanostructures,” *Applied Physics Letters* **118**, 012408 (2021).
- [23] Brian B. Maranville, Robert D. McMichael, and David W. Abraham, “Variation of thin film edge magnetic properties with patterning process conditions in Ni80Fe20 stripes,” *Applied Physics Letters* **90**, 232504 (2007).
- [24] Han-Jong Chia, Feng Guo, L. M. Belova, and R. D. McMichael, “Two-dimensional spectroscopic imaging of individual ferromagnetic nanostripes,” *Physical Review B* **86**, 184406 (2012).
- [25] Zhizhi Zhang, Michael Vogel, M. Benjamin Jungfleisch, Axel Hoffmann, Yan Nie, and Valentine Novosad, “Tuning edge-localized spin waves in magnetic microstripes by proximate magnetic structures,” *Physical Review B* **100**, 174434 (2019).
- [26] X. K. Hu, H. Dey, N. Liebing, H. W. Schumacher, G. Csaba, A. Orlov, G. H. Bernstein, and W. Porod, “Coherent precession in arrays of dipolar-coupled soft magnetic nanodots,” *Journal of Applied Physics* **117**, 243905 (2015).
- [27] J. Ding, M. Kostylev, and A. O. Adeyeye, “Broadband ferromagnetic resonance spectroscopy of permalloy triangular nanorings,” *Applied Physics Letters* **100**, 062401 (2012).
- [28] Justin M. Shaw, T. J. Silva, Michael L. Schneider, and Robert D. McMichael, “Spin dynamics and mode structure in nanomagnet arrays: Effects of size and thickness on linewidth and damping,” *Physical Review B* **79**, 184404 (2009).
- [29] A. F. Kravets, A. N. Timoshevskii, B. Z. Yanchitsky, M. A. Bergmann, J. Buhler, S. Andersson, and V. Korenivski, “Temperature-controlled interlayer exchange coupling in strong/weak ferromagnetic multilayers: A thermomagnetic Curie switch,” *Physical Review B* **86**, 214413 (2012).
- [30] A. F. Kravets, Yu. I. Dzhzherya, A. I. Tovstolytkin, I. M. Kozak, A. Gryshchuk, Yu. O. Savina, V. A. Pashchenko, S. L. Gnatchenko, B. Koop, and V. Korenivski, “Synthetic ferrimagnets with thermomagnetic switching,” *Physical Review B* **90**, 104427 (2014).
- [31] Dmytro Polishchuk, Yuliya Tykhonenko-Polishchuk, Vladyslav Borynskyi, Anatolii Kravets, Alexandr Tovstolytkin, and Vladislav Korenivski, “Magnetic hysteresis in nanostructures with thermally controlled RKKY coupling,” *Nanoscale Research Letters* **13**, 1–7 (2018).
- [32] B. C. Koop, T. Descamps, E. Holmgren, and V. Korenivski, “Relaxation-free and inertial switching in synthetic antiferromagnets subject to super-resonant excitation,” *IEEE Transactions on Magnetics* **53**, 1–5 (2017).
- [33] Erik Holmgren, Artem Bondarenko, Bjorn Koop, Boris Ivanov, and Vladislav Korenivski, “Non-degeneracy and effects of pinning in strongly coupled vortex pairs,” *IEEE Transactions on Magnetics* **53**, 1–5 (2017).
- [34] G. N. Kakazei, X. M. Liu, J. Ding, V. O. Golub, O. Y. Salyuk, R. V. Verba, S. A. Bunyayev, and A. O. Adeyeye, “Large four-fold magnetic anisotropy in two-dimensional modulated Ni80Fe20 films,” *Applied Physics Letters* **107**, 232402 (2015).
- [35] R. D. McMichael and M. D. Stiles, “Magnetic normal modes of nanoelements,” *Journal of Applied Physics* **97**, 10J901 (2005).
- [36] Arne Vansteenkiste, Jonathan Leliaert, Mykola Dvornik, Mathias Helsen, Felipe Garcia-Sanchez, and Bartel Van Waeyenberge, “The design and verification of MuMax3,” *AIP Advances* **4**, 107133 (2014).
- [37] Lukas Exl, Simon Bance, Franz Reichel, Thomas Schrefl, Hans Peter Stimming, and Norbert J. Mauser, “LaBonte’s method revisited: An effective steepest descent method for micromagnetic energy minimization,” *Journal of Applied Physics* **115**, 17D118 (2014).
- [38] A. F. Kravets, A. I. Tovstolytkin, Yu. I. Dzhzherya, D. M. Polishchuk, I. M. Kozak, and V. Korenivski, “Spin dynamics in a Curie-switch,” *Journal of Physics: Condensed Matter* **27**, 446003 (2015).
- [39] A. F. Kravets, D. M. Polishchuk, Yu. I. Dzhzherya, A. I. Tovstolytkin, V. O. Golub, and V. Korenivski, “Anisotropic magnetization relaxation in ferromagnetic multilayers with variable interlayer exchange coupling,” *Physical Review B* **94**, 064429 (2016).